arXiv:cond-mat/0405627v1 [cond-mat.mtrl-sci] 26 May 2004

Effect of anharmonicity of the strain energy on band offsets in semiconductor nanostructures

Olga L. Lazarenkova,[1,*] Paul von Allmen,[1] Fabiano Oyafuso,[1] Seungwon Lee,[1] and Gerhard Klimeck[1,2]

[1]*Jet Propulsion Laboratory, California Institute of Technology, Pasadena CA 91109*

[2]*Network for Computational Nanotechnology, School of Electrical and Computer Engineering, Purdue University, West Lafayette, IN 47906*

(Dated: May 25, 2004)

Anharmonicity of the inter-atomic potential is taken into account for the quantitative simulation of the conduction and valence band offsets for highly-strained semiconductor heterostructures. The anharmonicity leads to a weaker compressive hydrostatic strain than that obtained with the commonly used quasi-harmonic approximation of the Keating model. Inclusion of the anharmonicity in the simulation of strained InAs/GaAs nanostructures results in an improvement of the electron band offset computed on an atomistic level by up to 100 meV compared to experiment.

The accurate simulation of the electronic structure is of utmost importance for the design of nanoelectronic and optoelectronic device structures. It has been shown both theoretically[1,2] and experimentally[1,3,4,5], that the energy spectrum in semiconductor nanostructures is extremely sensitive to the built-in strain. Pryor *et al.*[2] has shown that the continuum elasticity method fails to adequately describe the strain profile in InAs/GaAs heterostructures with a 7% lattice mismatch between the constituent materials. The two-parameter valence-force-field (VFF) Keating model[6,7] is a commonly used approximation for atomistic-level calculations of the equilibrium atomic positions in realistic-size nanostructures[8]. This paper shows that the quasi-harmonic Keating model is insufficient to describe highly strained InAs/GaAs nanostructures, where anharmonicity of the strain energy becomes important.

Keating's model treats atoms as points connected with springs in a crystal lattice. The strain energy depends only the nearest-neighbor interactions within a quasi-harmonic approximation[6,7]:

$$E = \frac{3}{8}\sum_m\Bigg\{\sum_n\Big[\frac{\alpha_{mn}}{d_{mn}^2}(\mathbf{r}_{mn}\cdot\mathbf{r}_{mn}-\mathbf{d}_{mn}\cdot\mathbf{d}_{mn})^2 + \sum_{k>n}\frac{\sqrt{\beta_{mn}\beta_{mk}}}{d_{mn}d_{mk}}(\mathbf{r}_{mn}\cdot\mathbf{r}_{mk}-\mathbf{d}_{mn}\cdot\mathbf{d}_{mk})^2\Big]\Bigg\}. \quad (1)$$

The first coefficient, α, corresponds to the spring constant for the bond length distortion, while the second one, β, corresponds to the change of the angle between the bonds or, so-called, "bond-bending". Here the summation is over all m atoms of the crystal and their nearest neighbors n and k. $\mathbf{r}_{mn}$ and $\mathbf{d}_{mn}$ are the vectors connecting the m-th atom with its n-th neighbor in the strained and unstrained material, respectively.

A realistic interatomic potential is schematically shown in Fig. 1 with a line marked by large circles. The Keating interatomic potential corresponding to the Eq. (1) is plotted in Fig. 1 with dashed lines. The Keating potential is referred to as "quasi-harmonic" rather than "harmonic" since it depends upon the fourth rather than the second power of the bond length. This quasi-harmonic potential fails to reproduce the weakening of the interatomic interaction with increasing distance between atoms and it underestimates the repulsive forces at close atomic separation. Therefore Eq. (1) can adequately describe the strain energy only at small deformations. In the widely used InAs/GaAs heterostructures, the lattice mismatch is as large as 7% and anharmonicity of the interatomic potential is expected to become important.

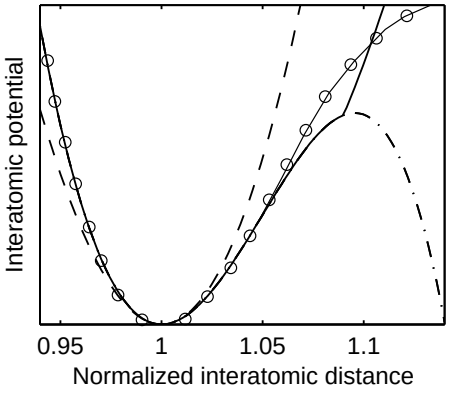

FIG. 1: Schematic interatomic potential used in the Keating (dashed line) and our model (solid line). Dash-dot line plot the model interatomic potential with the anharmonicity corrections to the VFF constants before the truncation. The line marked with large circles approximatly traces the shape of the realistic interatomic potential.

We include the anharmonicity of the interatomic potential directly into the Keating model by introducing distance-dependent VFF constants α and β:

$$\alpha_{mn} = \alpha_0^{mn}\Big[1-A_{mn}\frac{(r_{mn}^2-d_{mn}^2)}{d_{mn}^2}\Big], \quad (2)$$

$$\beta_{mnk} = \beta_0^{nmk}\Big[1-B_{nmk}(\cos\theta^{nmk}-\cos\theta_0^{nmk})\Big] \times\Big[1-C_{nmk}\frac{(r_{mn}r_{mk}-d_{mn}d_{mk})}{d_{mn}d_{mk}}\Big], \quad (3)$$

with the coefficients $\beta_0^{nmk}\equiv\sqrt{\beta_0^{mn}\beta_0^{mk}}$, $B_{nmk}\equiv\sqrt{B_{mn}B_{mk}}$, and $C_{nmk}\equiv\sqrt{C_{mn}C_{mk}}$. θ^{nmk} and θ_0^{nmk} are the actual and the unstrained angles between mn and mk bonds, respectively. In homogeneous mono-atomic and binary compounds, all bonds are the same and the indexes m, n, and k can be dropped. α_0 and β_0 are the VFF constants in the unstrained material. The anharmonicity correction coefficients A and C describe the dependence of bond-stretching and bond-bending forces on hydrostatic strain, while B is responsible for the change of the bond-bending term with the angle between bonds. The details of the derivation of the

anharmonicity corrections A, B, and C from the experimental phonon spectra of strained bulk materials are presented in Ref.[9]. The parameters used for the simulation of InAs/GaAs nanostructures are listed in Table I.

Material	α_0 (N/m)	β_0 (N/m)	A	B	C
GaAs	41.49	8.94	7.2	7.62	6.4
InAs	35.18	5.49	7.61	4.78	6.45

TABLE I: Valence-force-field constants in unstrained materials and anharmonicity correction coefficients for InAs and GaAs.

Introduction of the anharmonicity corrections in the VFF expression makes the form of the model potential more realistic and expands the validity range of the strain simulations (see Fig. 1). In order to ensure the convergence of the minimization of the energy (1) with α and β given by Eqs. (2), (3), our model inter-atomic potential was truncated as shown in Fig. 1 with the solid line. Note that the proposed introduction of the anharmonicity corrections in VFF constants does not substantially increase the computational time of the minimization of the total strain energy, since it does not introduce any additional summation in Eq. (1).

To illustrate the effect of the anharmonicity on the strain distribution in III-V semiconductor nanostructures, the hydrostatic, $\epsilon_H = 1/3(\epsilon_{xx} + \epsilon_{yy} + \epsilon_{zz})$, and biaxial, $\epsilon_B = 1/6(\epsilon_{xx} + \epsilon_{yy} - 2\epsilon_{zz})$, components of the strain in ultra-thin epitaxial InAs/GaAs layers have been computed using both the conventional Keating model and our model. The geometry of the structures and the obtained built-in strain are presented in Table II. Comparing the results of the two models, we note that the sharp rise of the strain energy at small inter-atomic distances leads to a smaller equilibrium hydrostatic compression than is obtained with the Keating model. At the same time, the quasi-harmonic approximation underestimates the bond stretching deformation. In contrast, biaxial compression is increased in our anharmonic model, while the biaxial tension is suppressed.

The band offsets for different InAs/GaAs nanostructures obtained for the strain distribution simulated within the Keating's model and including the anharmonicity corrections are compared with the available experimental data[3,4,5] in Table III. The local band structure was obtained within the $sp^3d^5s^*$ empirical tight-binding model where the Hamiltonian matrix elements depend on the distance between the atoms[10]. The tight-binding parameters were fitted to reproduce the properties both of the unstrained and strained bulk materials. Ultra-thin epitaxial layer structures[3,4] provide us with the perfect opportunity to test the effect of the anharmonicity at strong deformation on the valence and conduction band offsets. Anharmonicity corrections reduce the discrepancy between the experimental and modeled energies significantly (see Table III).

The strain distribution (Fig. 2, a, b) and the energy spectrum (Fig. 2, c) were computed for the quantum dot crystal (QDC) reported in Ref.[5]. The structure consists of three layers of *regimented* dome-shaped quantum dot arrays (with a 20 nm base diameter and a 7 nm height), vertically stacked with a small (3 nm) vertical separation between the QD layers. The 0.7 nm wetting layer is also included in our simulations to properly model the electronic spectrum[11]. The built-in strain distribution in such structures is very inhomogeneous. The average hydrostatical component of the strain tensor inside InAs quantum dots (Fig. 2, a) is overestimated by about 25% within the commonly used Keating model. At the same time, the biaxial strain distribution (Fig. 2, b) changes little when computed with the different models.

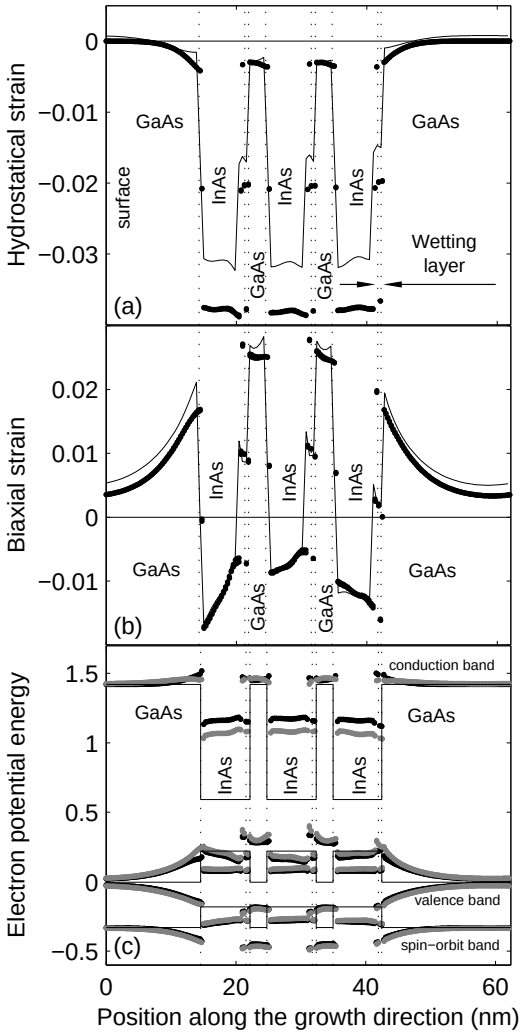

FIG. 2: Computed distribution of the hydrostatic (a) and biaxial (b) strain components, and (c) electronic band structure along the growth direction in InAs/GaAs QDC. The structure taken from Ref.[5] consists of three layers of dome-shaped QDs with a 20 nm base and a 7 nm height on top of the 0.7 nm wetting layer. The crossection is made near the center of the quantum dot stack. The results obtained with the Keating model are plotted with black dots. The results obtained with the anharmonic model are plotted with solid line on (a) and (b) and with gray dots on (c). The thin lines on (c) show the edges of conduction, valence, and spin-orbit split-off bands at the center of the Brillouin zone in the unstrained materials.

The main effect of the anharmonicity is a downward shift of the conduction band edge inside the quantum dots, as shown in Fig. 2, c. This is caused by the sensitivity of the conduction band to the hydrostatic compression, which is smaller within the anharmonicity model. The difference in the corresponding band edges obtained within the two models is as large

Ref.	x	y	Structure	Size L_x	Size L_y	Substr.	Hydrostatic strain (%) ϵ_H^K	Hydrostatic strain (%) ϵ_H^A	Hydrostatic strain (%) δ_H	Biaxial strain (%) ϵ_B^K	Biaxial strain (%) ϵ_B^A	Biaxial strain (%) δ_B
[3]	1.0	0.0	SQW	2 ML	5 ML	GaAs	-2.97	-2.59	14.9	-3.71	-4.10	-9.4
[3]	0.0	1.0	SQB	2 ML	5 ML	InAs	3.54	4.30	-17.7	3.72	2.90	28.3
[4]	1.0	0.0	MQW	1 ML	30 nm	GaAs	-2.87	-2.33	23.5	-3.81	-4.38	-13.0

TABLE II: Hydrostatic (H) and biaxial (B) strain components within the thin epitaxial layer in several structures computed within the Keating (K) model and taking into account the anharmonicity of the strain energy (A) for different $In_xGa_{1-x}As/In_yGa_{1-y}As$ nanostructures[3,4]. *Notations*: the nanostructure type: SQW – single quantum well, SQB – single quantum barrier, MQW – multiple quantum wells, ML – monolayer, L_x – width of the $In_xGa_{1-x}As$ epitaxial layer, L_y – width of the $In_yGa_{1-y}As$ epitaxial layer (corresponds to the thickness of the capping layer for SQW and SQB). $\delta = (\epsilon^K - \epsilon^A)/\epsilon^A$ shows the relative change of the computed built-in strain when the anharmonicity is neglected.

Ref.	Structure	Experimental method	ΔE_c (meV) K	δ_K (%)	A	δ_A (%)	Exp.	ΔE_v (meV) K	δ_K (%)	A	δ_A (%)	Exp.	Sub-band
[3]	SQW	XPS	471.5		574.0			374.6	-34.4	447.0	-15.7	530 ± 50	hh
[3]	SQB	XPS	-40.7		-91.3			-271.7	69.8	-225.9	41.2	-160 ± 50	lh
[4]	MQW	CV&DLTS	475.7	-31.1	584.4	-15.3	690	373.4		430.5			hh
[5]	QDC	DLTS	242.0	-29.0	347.0	1.8	341 ± 30						

TABLE III: Experimental band offsets in the conduction (ΔE_c) and valence (ΔE_v) bands compared with the offsets computed within the $sp^3d^5s^*$ empirical tight-binding model[10] using the equilibrium atomic positions found within the two-parameter Keating model (K) and including anharmonicity corrections to the VFF constants (A) for different $In_xGa_{1-x}As/In_yGa_{1-y}As$ nanostructures. The SQW, SQB, and MQW structures are the same as in Table II. The QDC structure[5] consists of three layers of dome-shaped QDs with a 20 nm base and a 7 nm height on top of a 0.7 nm wetting layer. The distance between the QD layers is about 10 nm. The band offsets are determined as the following: $\Delta E_c = E_c(In_yGa_{1-y}As) - E_c(In_xGa_{1-x}As)$ and $\Delta E_v = -(E_v(In_yGa_{1-y}As) - E_v(In_xGa_{1-x}As))$ so they would be positive for potential well and negative for potential barrier. *Notations*: the nanostructure type: SQW – single quantum well, SQB – single quantum barrier, MQW – multiple quantum wells, QDC – quantum dot crystal, i.e., the 3-dimensional *ordered* array of quantum dots; the band offset measurement techniques: XPS – X-ray photoemission spectroscopy, CV – capacitance-voltage spectroscopy, DLTS – deep-level transient spectroscopy. δ_K and δ_A estimate the relative deviations of the simulation from the experiment.

as 105.0 meV. This shift brings the overall band offset between the InAs quantum dot and GaAs buffer computed in our model very close to the experimentally observed value (see Table III). Due to the small difference in the biaxial strain distribution obtained with the two models (see Fig. 2, b), the energy structure of the valence band remains almost the same, as can be seen in Fig. 2, c.

In conclusion, we have demonstrated that the anharmonicity is important for the modeling of the electronic states in highly strained InAs/GaAs system. Compared to the standard Keating model we have found corrections of over 100 meV in some band offsets, resulting in values significantly closer to the experimental data. This demonstrates that the deformation in the nanostructures is beyond the applicability range of the quasi-harmonic approximation for the strain energy. The anharmonicity corrections can be performed without a significant increase of the computational cost, since the model remains limited to a nearest neighbour interactions.

Aknowledgements. The work described in this publication was carried out at the Jet Propulsion Laboratory, California Institute of Technology under a contract with the National Aeronautics and Space Administration. Funding was provided under grants from ARDA, ONR, JPL, NASA and NSF (Grant No. EEC-0228390). This work was performed while one of the authors (O.L.L.) held a National Research Council Research Associateship Award at JPL.

* Electronic address: Olga.L.Lazarenkova@jpl.nasa.gov

[1] J. Shumway, A. J. Williamson, A. Zunger, A. Passaseo, M. DeGiorgi, R. Cingolani, M. Catalano, and P. Crozier, *Phys. Rev. B* **64**, 125302 (2001).

[2] C. Pryor, J. Kim, L. W. Wang, A. J. Williamson, and A. Zunger, *J. Appl. Phys.* **83**, 2548 (1998).

[3] K. Hirakawa, Y. Hashimoto, K. Harada, and T. Ikoma, *Phys. Rev. B* **44**, 1734 (1991).

[4] R. Colombelli, V. Piazza, A. Badolato, M. Lazzarino, F. Beltram, W. Schoenfeld, and P. Petroff, *Appl. Phys. Lett.* **76**, 1146 (2000).

[5] S. Ghosh, B. Kochman, J. Singh, and P. Bhattacharya, *Appl. Phys. Lett.* **76**, 2571 (2000).

[6] P. N. Keating, *Phys. Rev.* **145**,2, 637 (1966).

[7] R. M. Martin, *Phys. Rev. B* **1**, 4005 (1970).

[8] L.-W. Wang, J. Kim, and A. Zunger, *Phys. Rev. B* **59**, 5678 (1999).

[9] O. L. Lazarenkova, P. von Allmen, F. Oyafuso, S. Lee, and G. Klimeck, *in preparation.*

[10] G. Klimeck, F. Oyafuso, T. B. Boykin, R. C. Bowen, and P. von Allmen, *CMES* **3**, 601 (2002). The NEMO3D software is available at `www.OpenChannelFoundation.org`

[11] S. Lee, O. L. Lazarenkova, F. Oyafuso, P. von Allmen, and G. Klimeck, `cond-mat/0405019`, submitted to *Phys. Rev. B*